Supporting Information

Development of Composite Alginate Bead Media with Encapsulated Sorptive Materials and Microorganisms to Bioaugment Green Stormwater Infrastructure

Debojit S. Tanmoy [a,b] and *Gregory H. LeFevre** [a,b]

[a] Department of Civil and Environmental Engineering, University of Iowa, 4105 Seamans Center, Iowa City, Iowa, 52242, United States

[b] IIHR—Hydroscience and Engineering, University of Iowa, 100 C. Maxwell Stanley Hydraulics Laboratory, Iowa City, Iowa, 52242, United States

*Corresponding Author:

gregory-lefevre@uiowa.edu; Phone: 319-335-5655; 4105 Seamans Center for Engineering, University of Iowa, Iowa City IA, United States

Contains: 13 total pages, 13 figures, and 2 tables.

Table of Contents

Section S 1. Stormwater Recipe and UIowa Water Treatment Process summary.

Synthetic stormwater Recipe: Synthetic stormwater was prepared using a previously described method by dissolving 0.072 mM of NH_4Cl, 0.75 mM of $CaCl_2$, 0.33 mM of Na_2SO_4, 0.072 mM of $NaNO_3$, 1 mM of $NaHCO_3$, 0.075 mM of $MgCl_2$, and 0.016 mM of Na_2HPO_4 in deionized water.[1]

UIowa Water Treatment Plant: UIowa-WP uses Iowa river water as an influent and distributes 900 million gallons of water annually.[2] The basic water treatment process in UIowa-WP includes but not limited to powdered activated carbon treatment, coagulation (currently using ferric chloride as coagulant), flocculation, sedimentation, lime softening, recarbonation, gravity filtration, and reverse osmosis.

Section S 2. Analytical Methods.

Bruanauer-Emmett-Teller (BET): A Quantachrome Nova 4200e BET instrument was used to determine the bead surface area and pore volume. All the samples were analyzed by the University of Iowa MATFab Facility (https://matfab.research.uiowa.edu), and the collected data were analyzed using the NovaWin software. BioSorp Bead samples were first inserted into glass tube sample holders with rod inserts and were then degassed at 90º C for 15 hours. The sample mass was recorded for later analysis. During analysis, the glass tube containing the samples was immersed in liquid nitrogen and a known quantity of ultra-pure nitrogen was introduced by the instrument for the nitrogen adsorption test. The bead surface area and the pore volume were quantified using the following BET equations[3] [**Equation 1**, **Equation 2**]:

Equation 1: $$\frac{x}{V(1-x)} = \frac{1}{(V_m)(C_{BET})} + \frac{x(C_{BET}-1)}{(V_m)(C_{BET})}$$

where V= volume of the adsorbed molecules, V_m= monolayer volume, C_{BET}= the BET constant, x= relative pressure (P/P0).

Equation 2: $$\text{Surface area} = \frac{(V_m)(N_A)(a_m)}{(V_m)(m_s)}$$

where N_A= Avogadro's number (6.022×10^{23} mol^{-1}), a_m= effective cross-section area of one adsorbed molecule, v_m= molar volume of one adsorbed molecule, m_s= mass of the adsorbent.

Atomic Force Microscope (AFM): Stiffness of the beads was quantified using a Molecular Force Probe 3D Classic (MFP-3D) Atomic Force Microscope (Asylum Research, Santa Barbara, CA, USA). Young's moduli were measured on multiple positions for each bead to obtain the representative average bead mechanical strength. All AFM studies were conducted by the Tivanski group at the Department of Chemistry, University of Iowa and using previously established AFM protocols.[4–6] All AFM experiments were performed at room temperature and pressure. The force analysis was conducted using MikroMasch CSC37 silicon nitride probes (nominal spring constant= ~1.0 N/m; tip radius of curvature= 10 nm; scan rate= 1 Hz). Thermal noise method was used to determine the actual AFM tip spring constant. A humidity cell was used to control the relative humidity (RH) and an intermittent contact mode (AC mode) was used to generate the AFM height images at that specific RH. Whenever the RH changed, 10 to 15 minutes of equilibration time was allotted to ensure thermodynamic balance.

Scanning Electron Microscope (SEM), Stereoscope, and ICP-MS: Closeup surface images of the beads were taken using Hitachi S-4800 Scanning Electron Microscope. All the samples were run by the Central Microscopy Research Facility (CMRF, https://cmrf.research.uiowa.edu/) at the University of Iowa. Dried samples were placed on adhesive carbon coated aluminum stubs. The

stubs were sputter-coated with gold and palladium (60:40) prior to the imaging steps. An Olympus SZX12 Stereoscope at the CMRF was used to image fungal growth from the beads. Agilent 7900 ICP-MS was used to measure dissolved phase Ca^{2+} and Fe^{3+} concentrations for the leaching experiment.

Figure S 1. Calcium alginate beads (made with sodium alginate, PAC, wood flour, Fe-WTR, calcium chloride) [left] and Iron (III) alginate beads (made with sodium alginate, PAC, wood flour, Fe-WTR, Ferric chloride) [right]. Final dried beads (~3mm) decrease in diameter by approximately half from the wet size; coin shown for size reference is a US Quarter.

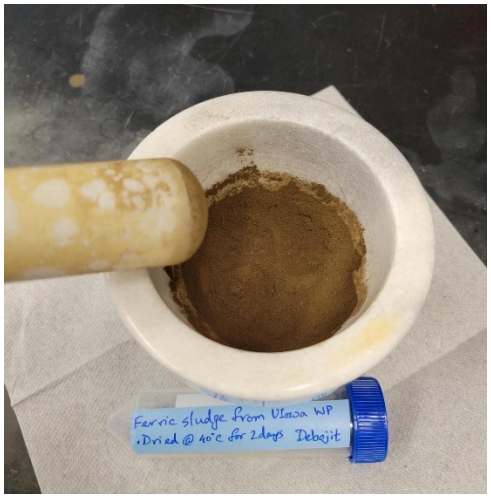

Figure S 2. Powdered iron water treatment residuals (Fe-WTR).

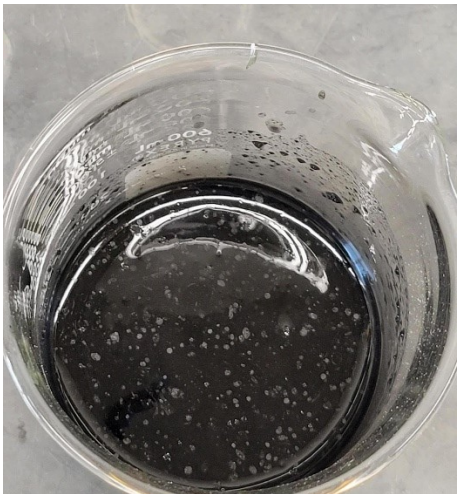

Figure S 3. Mixture of sodium alginate, PAC, wood flour, Fe-WTR, and fungi.

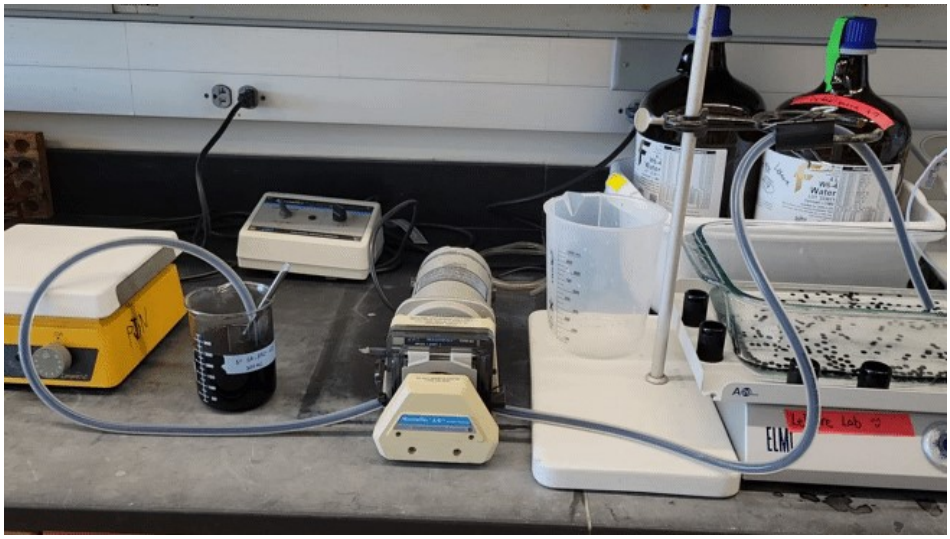

Figure S 4. BioSorp Bead making process. PAC, wood flour, Fe-WTR, and white rot fungi culture are mixed thoroughly in a beaker [left]. The mixture is then pumped using a peristaltic pump and dropped into a crosslinking solution (in this case, calcium chloride) [right]. The crosslinking solution is continuously shaken on a platform shaker such that the formed beads do not stick to each other.

Figure S 5. Bead formation in calcium chloride solution. The wet beads are approximately 6 mm in diameter.

Figure S 6. Wet BioSorp Beads being air-dried on wax paper.

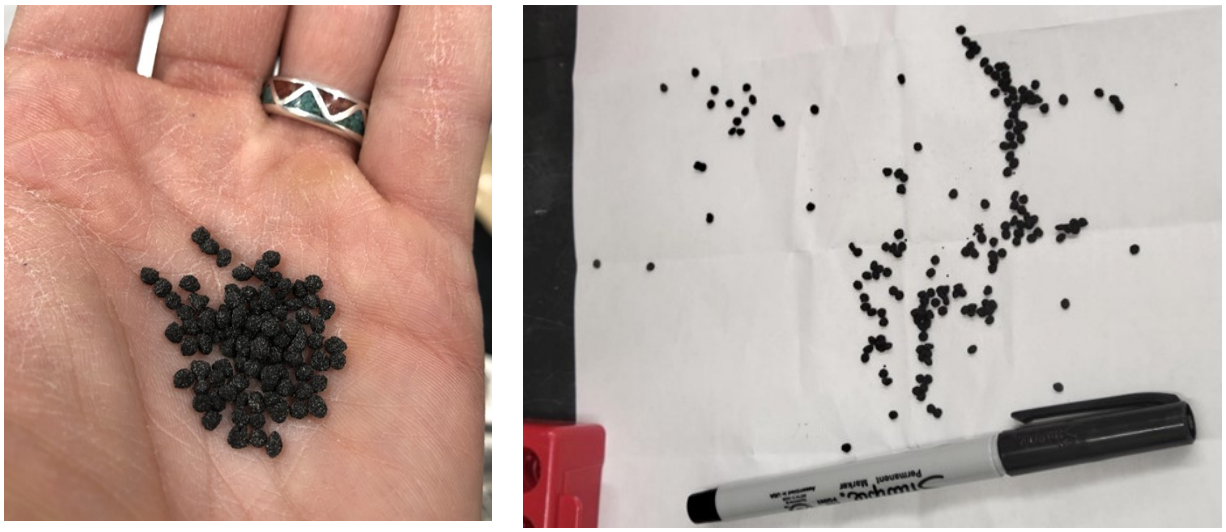

Figure S 7. Dried BioSorp beads in palm of the hand (left) and on wax paper (right).

Figure S 8. Making of PAC-wood flour beads with sodium alginate and ferric chloride.

Figure S 9. Air drying PAC-wood flour beads on wax paper.

Figure S 10. Precipitated iron from Ferric-alginate beads in synthetic seawater.

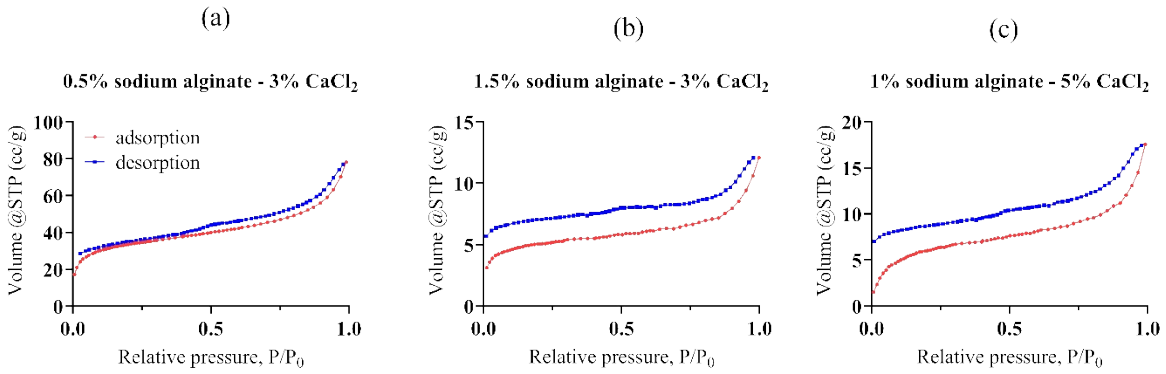

Figure S 11. BET adsorption isotherms for three types of beads- (a) 0.5% sodium alginate- 1% PAC-1% wood flour-3% $CaCl_2$, (b) 1.5% sodium alginate- 1% PAC-1% wood flour-3% $CaCl_2$, and (c) 1% sodium alginate- 1% PAC-1% wood flour-5% $CaCl_2$.

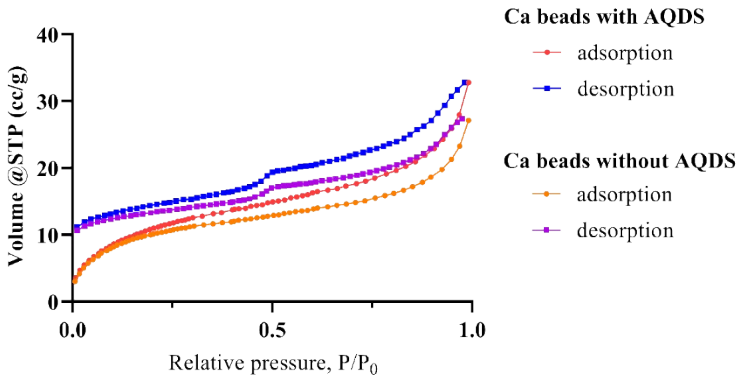

Figure S 12. BET adsorption isotherms for two types of Ca beads- type 1: contains AQDS (1% sodium alginate- 1% PAC-1% wood flour-1% FeWTR- 3% $CaCl_2$) and type 2: does not contain AQDS (1% sodium alginate- 1% PAC-1% wood flour-1% FeWTR-3% $CaCl_2$).

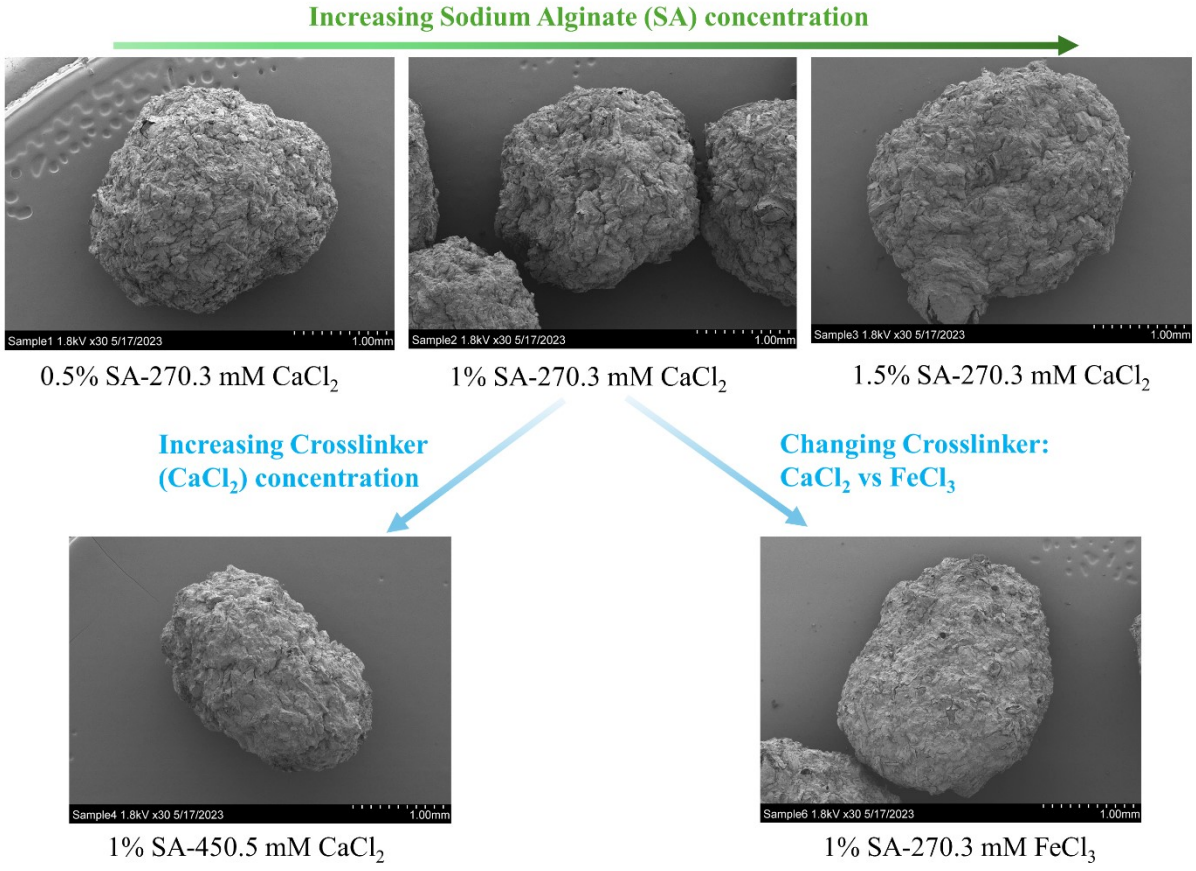

Figure S 13. SEM images of different composite alginate beads (scale bar= 1 mm).

Table S 1. Testing the impacts of different BioSorp Bead production conditions on various measured properties.

Testing conditions for characterization		Bead Preparation Recipe								Measured Bead Properties	Descriptive Impacts on Measured Properties
		Sodium Alginate Concentration	Crosslinker Concentration	Cross-linker Type	External Electron Shuttle (AQDS)	PAC	Wood Flour	Fe-WTR	Drying Temperature		
1. Varied Alginate Concentration	**Baseline condition**	**1%**	270.3 mM	$CaCl_2$	-	1%	1%	-	Air dried at room temp	Surface area; Total pore volume	Surface area and pore volume **decreases** with the increase in alginate
	Other conditions	**0.5%, 1.5%**	270.3 mM	$CaCl_2$	-	1%	1%	-	Air dried at room temp		
2. Varied Cross-linker Concentration	**Baseline condition**	1%	**270.3 mM**	$CaCl_2$	-	1%	1%	-	Air dried at room temp	Surface area; Total pore volume	Surface area and pore volume **decreases** with the increase in
	Other conditions	1%	**450.5 mM**	$CaCl_2$	-	1%	1%	-	Air dried at room temp		
3. Varied Cross-linker Type	**Baseline condition**	1%	270.3 mM	**$CaCl_2$**	-	1%	1%	-	Air dried at room temp	Surface area; Total pore volume	Crosslinking with **$FeCl_3$ increases** surface area and pore volume
	Other conditions	1%	270.3 mM	**$FeCl_3$**	-	1%	1%	-	Air dried at room temp		
4. Effects of External Electron Shuttle	**Baseline condition**	1%	270.3 mM	$CaCl_2$	-	1%	1%	1%	Air dried at room temp	Surface area; Total pore volume	Addition of AQDS **marginally decreases** surface area and pore
	Other conditions	1%	270.3 mM	$CaCl_2$	**0.1%**	1%	1%	1%	Air dried at room temp		
5. Effects of Cross-linker Type on Mechanical	**Baseline condition**	1%	270.3 mM	**$CaCl_2$**	0.1%	1%	1%	1%	Air dried at room temp	Mechanical Strength	Crosslinking with **$FeCl_3$ increases** bead strength
	Other conditions	1%	270.3 mM	**$FeCl_3$**	0.1%	1%	1%	1%	Air dried at room temp		
6. Drying Temperature	**Baseline condition**	1%	270.3 mM	$CaCl_2$	0.1%	1%	1%	1%	**Air dried at room temp**	Fungal viability	**Similar** fungal viability
	Other conditions	1%	270.3 mM	$CaCl_2$	0.1%	1%	1%	1%	**Oven dried (at 70° C for 8 hours)**		

Table S 2. Dissolved Ca and dissolved Fe concentrations in DI water, synthetic stormwater, 10X synthetic stormwater, 20X synthetic stormwater, and synthetic seawater (values that were not measured are shown with hyphen).

	Day	DI water	SW (Ionic strength= 0.005 M)	10X SW (Ionic strength= 0.05 M)	20X SW (Ionic strength= 0.1 M)	Seawater (Ionic strength= 0.7 M)	Note
Dissolved Ca (mg/L)	0	0.728	47.1276	285.9766	572.7462	337.2148	Ca beads were kept in the solvents
	22	57.525	69.5994	327.925	610.4254	408.356	
	42	62.7484	79.6198	-	-	-	
Dissolved Fe (mg/L)	0	0.0026	<0.0000	-	-	<0.0000	Fe beads were kept in the solvents
	22	3.3592	0.1768	-	-	<0.0000	
	42	2.9484	0.1014	-	-	-	

References:

1 J. M. Wolfand, G. H. LeFevre and R. G. Luthy, Metabolization and degradation kinetics of the urban-use pesticide fipronil by white rot fungus Trametes versicolor, Environ. Sci.: Processes Impacts, 2016, 18, 1256–1265.

2 University of Iowa, Water Production and Filtration, https://facilities.uiowa.edu/drinking-water-quality, (accessed 12 May 2024).

3 M. Naderi, ed. S. B. T.-P. in F. and S. Tarleton, Academic Press, Oxford, 2015, pp. 585–608.

4 C. P. Kaluarachchi, V. W. Or, Y. Lan, C. K. Madawala, E. S. Hasenecz, D. R. Crocker, C. K. Morris, H. D. Lee, K. J. Mayer, J. S. Sauer, C. Lee, G. Dorce, F. Malfatti, E. A. Stone, C. D. Cappa, V. H. Grassian, K. A. Prather and A. V Tivanski, Size-Dependent Morphology, Composition, Phase State, and Water Uptake of Nascent Submicrometer Sea Spray Aerosols during a Phytoplankton Bloom, ACS Earth Space Chem, 2022, 6, 116–130.

5 C. P. Kaluarachchi, V. W. Or, Y. Lan, E. S. Hasenecz, D. Kim, C. K. Madawala, G. P. Dorcé, K. J. Mayer, J. S. Sauer, C. Lee, C. D. Cappa, T. H. Bertram, E. A. Stone, K. A. Prather, V. H. Grassian and A. V Tivanski, Effects of Atmospheric Aging Processes on Nascent Sea Spray Aerosol Physicochemical Properties, ACS Earth Space Chem, 2022, 6, 2732–2744.

6 C. K. Madawala, H. D. Lee, C. P. Kaluarachchi and A. V Tivanski, Probing the Water Uptake and Phase State of Individual Sucrose Nanoparticles Using Atomic Force Microscopy, ACS Earth Space Chem, 2021, 5, 2612–2620.